行政院國家科學委員會專題研究計畫　成果報告

局部與全面性形變應力矽通道金氧半電晶體之特性與可靠度分析

計畫類別：個別型計畫
計畫編號：NSC94-2215-E-009-065-
執行期間：94 年 08 月 01 日至 95 年 07 月 31 日
執行單位：國立交通大學電子工程學系及電子研究所

計畫主持人：黃調元

計畫參與人員：林宏年、呂嘉裕、盧景森、謝雨霖、趙志誠、黃健銘

報告類型：精簡報告
報告附件：出席國際會議研究心得報告及發表論文
處理方式：本計畫可公開查詢

中　華　民　國 95 年 10 月 13 日

行政院國家科學委員會補助專題研究計畫 ■ 成 果 報 告
□期中進度報告

局部與全面性形變應力矽通道金氧半電晶體之特性與可靠度分析

Characteristics and Reliability of Local and Global Strained-Si Channel MOSFET

計畫類別：■ 個別型計畫　　□ 整合型計畫
計畫編號：NSC 94－2215－E－009－065
執行期間：94 年 08 月 01 日 至 95 年 07 月 31 日

計畫主持人：黃調元 教授
計畫參與人員： 林宏年、呂嘉裕、盧景森、謝雨霖、趙志誠、黃健銘

成果報告類型(依經費核定清單規定繳交)：■精簡報告　□完整報告

本成果報告包括以下應繳交之附件：
□赴國外出差或研習心得報告一份
□赴大陸地區出差或研習心得報告一份
□出席國際學術會議心得報告及發表之論文各一份
□國際合作研究計畫國外研究報告書一份

處理方式：除產學合作研究計畫、提升產業技術及人才培育研究計畫、列管計畫及下列情形者外，得立即公開查詢
□涉及專利或其他智慧財產權，□一年□二年後可公開查詢

執行單位：國立交通大學電子工程研究所

中　華　民　國　　年　　月　　日

局部與全面性形變應力矽通道金氧半電晶體之特性與可靠度分析

"Characteristics and Reliability of Local and Global Strained-Si Channel MOSFET"

計畫編號：NSC94-2215-E-009-065

執行期間：94 年 8 月 01 日 至 95 年 7 月 31 日

主持人：黃調元 交通大學電子工程系教授

中文摘要

在本報告中，將探討具有氮化矽覆蓋層之形變應力 N 型通道金氧半場效電晶體之特性。雖然氮化矽覆蓋層能大大增強載子遷移率以及提高元件之驅動電流，但是同時也犧牲了熱載子可靠度，主要是沉積氮化矽覆蓋層之過程中，大量的氫擴散進去元件通道中。即使氮化矽覆蓋層之後移除掉，釋放了通道形變應力，但是熱載子劣化依舊比沒有氮化矽覆蓋層之元件來的嚴重。最後，經由熱載子劣化測試產生之介面能態側向分佈也將在本計畫中探討。

關鍵字：氮化矽覆蓋層、伸張應力、熱載子劣化、介面能態側向分佈。

Abstracts

Characteristics of strain channel nNMOSFETs with SiN capping layer were investigated in this work. Although the incorporation of the SiN capping layer could dramatically enhance the carrier mobility and thus the drive current of the fabricated devices, the resistance to hot-carrier degradation is sacrificed as well, owing to the high hydrogen contents in the SiN layer which might diffuse to the channel region during the process. Even if the SiN layer is removed and the channel strain released later, the hot carrier degradation remains severer than devices without SiN capping. Finally, lateral distribution of generated interface states due to hot-carrier stressing was also investigated in this study.

Keywords: SiN capping, tensile strain, hot carrier stress (HCS), lateral distribution of interface state.

Introduction

Channel strain engineering improves the drive current of MOSFETs by fundamentally altering the band structure of the device channel and can therefore enhance the performance of aggressively scaled devices [1-3]. With the performance improvement being demonstrated, attentions should now be paid to the associated reliability issues for practical applications. Currently, device degradation caused by hot electrons represents one of the most critical reliability issues in deep sub-micron NMOSFETs [4,5]. Although the physical mechanisms and characteristics of hot electron degradation have been extensively examined [6,7], there seems to be very few works that investigate the impact of SiN capping layer and the associated deposition process on the hot carrier reliability of the strained devices. In this work, we investigate hot carrier degradation characteristics of NMOS devices having local channel strain induced by a SiN-capping layer.

Experimental

The NMOSFETs used in this study were with 3 nm thermal oxide and 150 nm poly-Si layer as the gate electrode. After the gate formation, most samples were capped with a SiN layer of 300 nm, deposited by a LPCVD system (denoted as the SiN-capped split), while some wafers were deliberately skipped of the SiN deposition to serve as the controls (denoted as the control split). The SiN deposition was performed at 780˚C with SiH_2Cl_2 and NH_3 as the reaction precursors. The SiN layer was deliberately removed after deposition from some of the SiN-capped samples in order to evaluate the impact of SiN deposition process itself on the device performance (denoted as SiN-removal split).

The lateral diffusion of interface state after hot carrier stress for all splits was also evaluated in this work based on the method developed in [8] and the measurement setup is shown in Fig. 1. The experimental procedures of this method are briefly described below:

(1) Measure the Icp-V_h curve on a virgin MOSFET from the drain junction (with the source junction floating), and from it establish the V_h versus $V_{th}(x)$ relationship [9] near the junction of interest.

(2) Re-measure the Icp-V_h curve after hot-carrier injection.

(3) Obtain the hot-carrier-induced interface state distribution, $N_{it}(x)$, from the difference of the Icp-V_h curve before and after hot carrier stress.

Results and Discussion

Figure 2 shows the percentage increase of the drive current for the SiN-capped and SiN-removal samples compared with the controls, as a function of channel length. The drive current enhancement reaches about 20% at a channel length of 0.4 μm in the SiN-capped sample. On the other hand, the SiN-removal device shows negligible enhancement. These observations demonstrate that the current enhancement is truly due to the uniaxial tensile strain induced by the SiN capping which increases with decreasing channel length.

The impact ionization rate (I_{sub}/I_d) of the fabricated devices is shown Fig. 3. It is clearly seen that I_{sub}/I_d is much larger in the SiN-capped device, as compared with the other two splits. This result indicates that the channel strain plays an important role in affecting the generation of channel hot electrons and the associated impact ionization process. This could be related to the bandgap narrowing effect induced by the channel strain as well as the increased mobility, both tend to enhance the impact ionization rate [10,11], and may potentially worsen the hot-electron degradation in the strained devices. In Fig. 3, it is also interesting to note that I_{sub}/I_d in the SiN-removal samples is also larger than the control. This could be explained by the additional thermal budget and hydrogen species by the SiN deposition process that tend to reduce the implant damage located close to the drain region. Figure 4 shows ΔV_{th} and ΔN_{it} as a function of the stress time. As mentioned above, the device with channel strain depicts aggravated degradation in terms of larger shifts in these parameters. Figure 5 illustrates the 10-year reliability projections for the three splits. Lifetime was defined as 30 mV of ΔV_{th}. Devices with SiN capping were observed to endure lower

V_{DS} as compared with the control and SiN-removal samples. Because of extra hydrogen species, the SiN-removal devices show worse lifetime than the control ones.

The measurement presented in Fig. 1 was used to extract lateral diffusion of interface states after hot carrier stress. First, Fig. 6 shows the local V_{th} versus distance x of all splits. Basically, the lateral doping profile is nearly the same, except for the difference in local V_{th}. The variation of V_{th} is due to bandgap narrowing induced by the strained-channel. Moreover, the local V_{th} decreases sharply as x is smaller than 0.07 μm. We can approximately speculate that the drain junction is near x = 0.07 μm. The derived profiles of the interface state lateral diffusion are shown in Fig. 7 after 100 sec hot carrier stress. One can see that the damage region is confined within 0.1μm from the drain in all splits. In addition, the aggravated hot carrier stress of the SiN-removal devices is presumably due to the extra hydrogen species that may pile up at the source/drain edge during the SiN deposition. This explains why the SiN-removal devices show larger generation rate of interface state than control devices.

Conclusions

Both the presence of the SiN capping layer and the deposition process itself exert significant impacts on the device operation and the associated reliability characteristics. The accompanying bandgap narrowing and the increased carrier mobility tend to worsen the hot-electron reliability. This work shows that hot-electron degradation is adversely affected when the SiN layer is deposited over the gate, even if the SiN layer is removed later and the channel strain is relieved. Owing to the use of hydrogen-containing precursors, abundant hydrogen species is incorporated in the oxide that may also contribute to the hot-electron degradation. The edge effect of hot carrier stress is also an important factor that causes degraded reliability in SiN-removal devices.

References

[1] M. Lee et al., JAP, 2005, p.011101-1.

[2] V. Chan et al., in Tech. Dig. of IEDM, 2003, p.77.

[3] S.E. Thompson et al., IEEE ED Lett.,2004, p.191.

[4] E. Li et al., IEEE Trans. on ED, 2001, p.671.

[5] H. S. Momose et al., in Tech. Dig. of IEDM, 1997, p.453.

[6] A. Schwerinet al., IEEE Trans. on ED, 1987, p.2493.

[7] P. Heremans et al., IEEE Trans. on ED, 1988, p.2194.

[8] C. Chen et al., IEEE Trans. on ED, 1998, p.512.

[9] M. Tsuchiaki et al., IEEE Trans. on ED, 1993, p.1768.

[10] N. Sano eta al., IEEE Trans. on ED, 1995, p.2211.

[11] M. F. Lu et al., IRPS, 2004, p.18.

此計畫之論文發表

1. VLSI Tech., 2005, pp.174.
2. EDL-26 (9), 2005, pp.676.
3. ECSL-9, 2006, pp.138
4. JJAP-45, 2006, pp.3064
5. EDL-27 (8), 2006, pp.659
6. SSDM, 2006, pp. 528

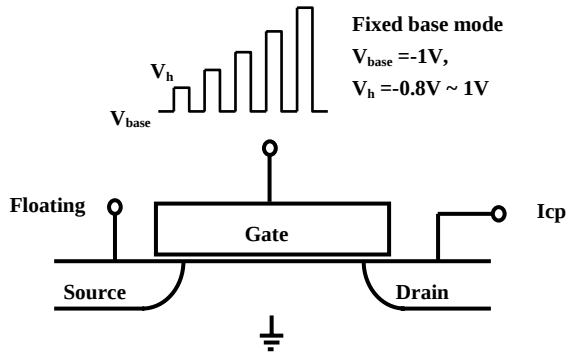

Fig.1. Measurement setup of single junction charge pumping measurement.

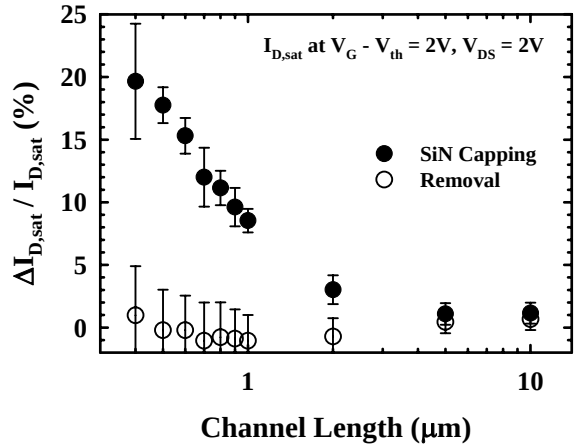

Fig.2. Saturation current increase versus channel length. The saturation current was defined at $V_G - V_{th}$ = -2 V and V_{DS} = -2 V

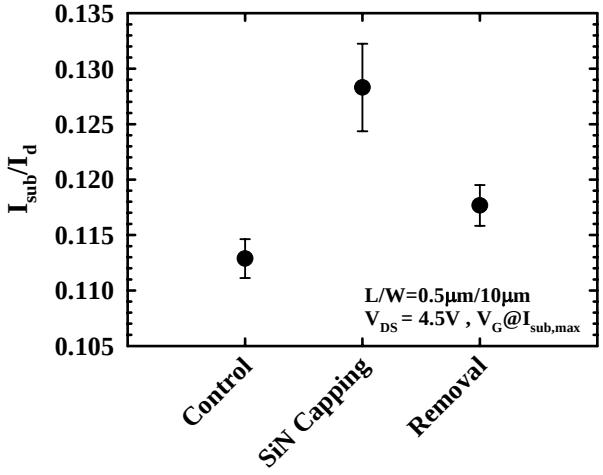

Fig.3 The impact ionization rate (I_{sub}/I_d) in all splits.

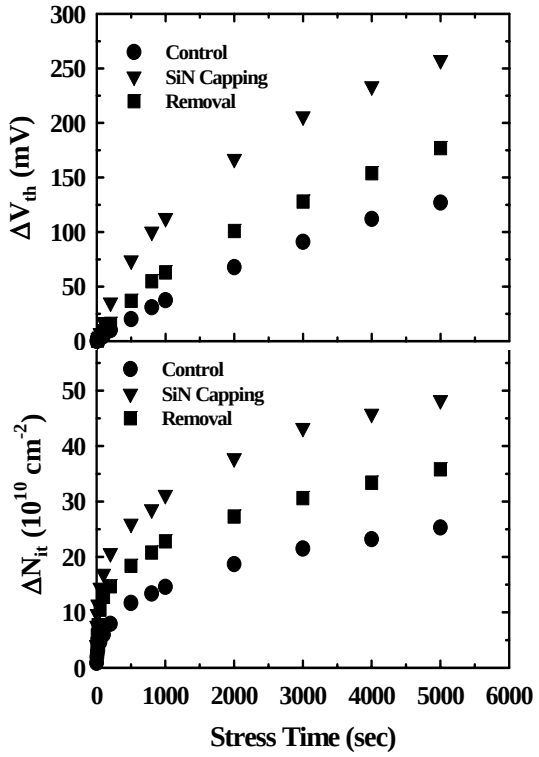

Fig. 4 Results of hot-electron stressing at V_{DS} = 4.5 V and maximum substrate current performed on all three splits of with channel length/width = 0.5μm/10μm. (a) Threshold voltage shift. (b) Interface state generation.

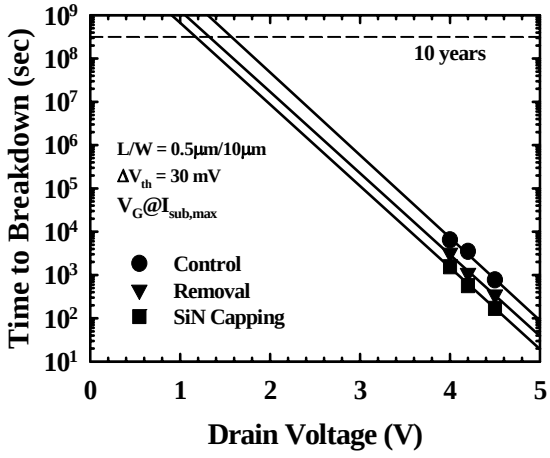

Fig. 5 The 10-year lifetime projection for the control, SiN-removal, and SiN-capped samples.

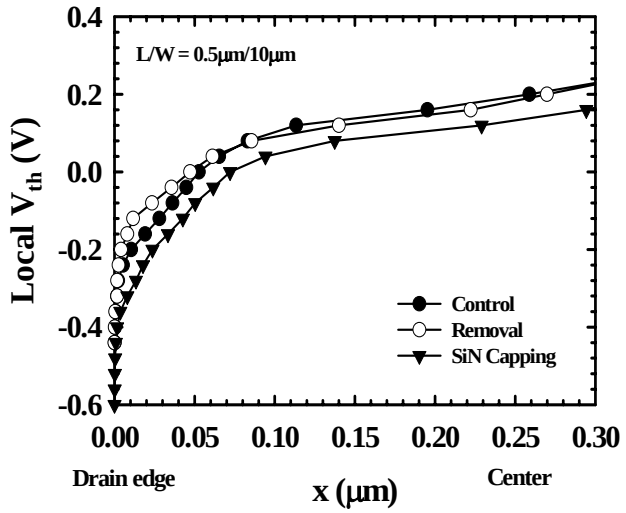

Fig. 6 The derived lateral profile of local threshold voltage near the graded drain junction.

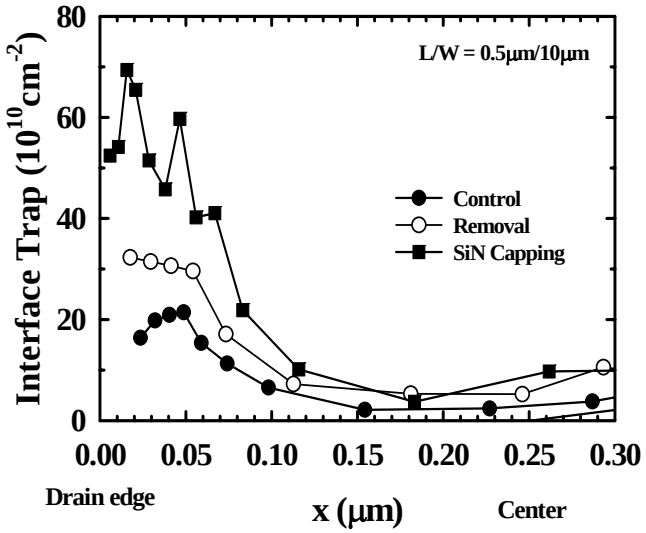

Fig. 7 Lateral profile of interface state generation after hot carrier stress of all splits.